Desalination and Water Treatment
www.deswater.com

doi: 10.5004/dwt.2020.26006

197 (2020) 358–367
September

Removal of methylene blue dye from water with low cost *Nigella sativa* seeds waste: kinetic, isotherm, and statistical modeling

Dounia Sid[a,b], Yahia Salem[a], Milad Baitiche[b], Ferhat Djerboua[b], Nadia Boukhalfa[a], Mokhtar Boutahala[a,*]

[a]*Laboratory of Chemical Process Engineering, Department of Process Engineering, Faculty of Technology, University of Ferhat Abbas Setif-1, 19000 Setif, Algeria, Tel. +213 36-83-49-74; Fax: +213-36-83-74; emails: mboutahala@yahoo.fr (M. Boutahala), douniasid3005@gmail.com (D. Sid), salamyahia@gmail.com (Y. Salem), nadouchette2011@hotmail.fr (N. Boukhalfa)*
[b]*Laboratory of Multiphasic and Polymeric Materials, Department of Process Engineering, Faculty of Technology, University of Ferhat Abbas Setif-1, 19000 Setif, Algeria, emails: baitiche_milad@yahoo.fr (M. Baitiche), ferhatdjerbouaf@gmail.com (F. Djerboua)*

Received 12 December 2019; Accepted 17 April 2020

ABSTRACT

Nigella sativa seeds waste (NSW) was characterized by Fourier transformed infrared spectroscopy, X-ray diffraction, thermogravimetric analysis-TDA, and scanning electron microscopy analysis and used for the adsorptive uptake of methylene blue (MB) from water. The specific surface area of NSW determined by the methylene blue adsorption method was equal to 465.95 m²/g. The experimental equilibrium data were investigated using the isotherm equations of Langmuir, Freundlich, Temkin, Redlich–Peterson, Sips, and Radke–Prausnitz. The models of pseudo-first-order, pseudo-second-order, Elovich, intraparticle diffusion, and Avrami were applied for the kinetic data modeling. The maximum MB adsorption capacity of NSW obtained by the Langmuir equation was 149.4 mg/g. The experimental kinetic data fitted very well to the Avrami model. Thermodynamic parameters indicate the spontaneous and endothermic nature of MB adsorption onto NSW. The statistical physics model with single energy was used to determine the adsorption mechanism of MB on NSW. The model confirms the endothermic and physical nature of the process with an anchorage of MB onto NSW. The receptor site density (N_M), the adsorbed dye quantity at saturation (N_{sat}), the concentration at half-saturation ($C_{1/2}$) and the adsorption energy (ΔE) values are equal to 128.23, 141.1 mg/g, 25.4 mg/L and 18.0 kJ/mol, respectively.

Keywords: Agro-wastes; Adsorption; Low cost adsorbent; Dye; Methylene blue; Statistical physics

1. Introduction

Organic dyes are widely used in many industrial sectors [1]. They can be divided into natural and synthetic dyes. They are responsible for water coloring and can reduce light penetration and subsequently photosynthesis in it. On the other side, because of their toxicity and dangerousness, dyes can also affect human health and safety. Therefore, the elimination of these products from water has become one of the major issues in water treatment.

Several water depollution methods such as advanced oxidation, photocatalytic oxidation/degradation, and membrane separation have been effectively applied for the elimination of different dyes from water, but most of them are expensive and require energy or produce huge quantities of sludge and generate derivatives that are sometimes more toxic than the dyes themselves.

Among the favorable processes for treating water polluted with dyes is adsorption, which proves to be an effective method [2–8]. Activated carbon is one of the most used adsorbents on this subject. However, the cost of

* Corresponding author.

activation can be quite high sometimes [9], which may be due to the use of non-renewable and relatively expensive starting materials such as coal.

Recently, numerous studies were carried out for the preparation of inexpensive adsorbent materials using cheap precursors available locally from renewable natural sources such as agricultural solid wastes. Agricultural residues are generally rich in cellulose, hemicellulose, and lignin. Their surfaces contain specific functional groups such as alcohol, phenol, aldehyde, carboxyl, and ketone, which may help in the removal of various pollutants by adsorption. A large number of agricultural wastes such as agave bagasse, corncob, peels of garlic, potato, and banana, have been investigated for dyes adsorption [10,11].

Nigella sativa seed (NSS) is an annual flowering plant in the family of *Ranunculaceae*. It is widely used in the Mediterranean and North African countries [12]. The oil of NSS has been traditionally used for several treatments such as infertility, fever, cough, and chronic headache [13]. It was also used in phytotherapy and alternative medicine [14,15]. The extraction of NSS oil generates hundreds of tons of wastes that are generally used in agriculture as a fertilizer or as a dietary supplement for animal breeding. The conversion of these wastes to a bioadsorbant for dyes seems to be an interesting application since they are biodegradable and cheap materials. In this context, NSW was tested as a low cost and ecofriendly adsorbent for the removal of MB from water under the influence of the solution pH, contact time, initial MB concentration, and NSW dose. The mechanism of MB adsorption onto NSW surface was not well explained in the literature. Thus, a good explanation of the adsorption results using various isotherm and kinetic models was given in this study. In addition, the monolayer adsorption model derived by statistical physics was also used to attribute geometric and energetic interpretations of the MB adsorption process.

2. Experimental

2.1. Materials and methods

Methylene blue ($C_{16}H_{18}N_3SCl$) (color index 52015, λ_{max} = 665 nm, MW = 319.8 g/mol, pKa = 5.6 [16]) was purchased from Sigma-Aldrich (France). NSS waste was obtained after the extraction of the NSS oil. The waste was washed several times with deionized water to remove impurities and dried at 50°C for 24 h. The obtained solid was than the ground, sieved, and directly characterized and investigated in adsorption experiments.

2.2. Characterization techniques

Moisture, ash, volatile matter, and fixed carbon content in NSW samples were obtained according to ASTM D 3172–3175 standards (ASTM 1999). X-ray diffraction (XRD) analysis of NSW was performed by X'PertPro (France) diffractometer with CuKα = 1.54 Å in the 2θ range of 10°–80°. The infrared spectra of NSW before and after MB adsorption were obtained using (Fourier transformed infrared spectroscopy) FTIR-8400S Shimadzu (Japan) spectrophotometer from 400 to 4,000 cm^{-1}. The morphology of the NSW surface before and after MB adsorption was characterized by JCM-5000 NeoScope scanning electron microscopy (SEM). Thermal analysis of NSW was recorded in Sdt Q600 V20 9 build 20 thermal gravimetric instruments under the nitrogen atmosphere (flow rate 100 mL/min) at a heating rate of 10°C/min. The isoelectric point (pH_{PZC}) was determined in MB solution by the pH drift method [17] in the range of pH 2–12 using HCl and NaOH solutions. The specific surface area of NSW was determined by the methylene blue adsorption method [18], and calculated from the following equation:

$$S_{MB}(m^2/g) = \frac{\left(q_{max} \times A_{MB} \times N_A \times 10^{-3}\right)}{MW} \quad (1)$$

where S_{MB} is the specific surface area determined using MB as adsorbate (m^2/g), q_{max} is the maximum adsorption capacity (mg/g), A_{MB} is the occupied area by a molecule of MB (175.2 $Å^2$), N_A is the Avogadro's number (6.023×10^{23}), and MW is the molecular weight of MB (319.8 g/mol).

2.3. Adsorption experiments

All experimental effects on MB adsorption were carried out using 50 mL of MB solution of concentration equal to 10 mg/L and 50 mg of NSW under stirring rate of 150 rpm at T = 20°C ± 1°C for 2 h. The pH effect was investigated in the pH range of 2–12. The effect of the adsorbent masse was studied by varying the adsorbent weight from 10 to 160 mg at pH = 6.7 (the pH of MB solution). The thermodynamic studies were carried out from 20°C to 40°C.

The kinetic batch tests were carried out at MB concentration from 10 to 60 mg/L. After the determined contact time, each mixture was centrifuged and the amount of adsorbed MB was calculated by Eq. (2) after UV-vis spectrophotometric measurements.

$$q_t = \frac{\left(C_0 - C_t\right) \times V}{m} \quad (2)$$

where q_t is the adsorbed MB (mg/g) at time t, C_0 is the initial concentration of MB (mg/L), C_t is the concentration at time t (mg/L), V is the volume of the solution (mL), and m is the mass of the adsorbent (g).

For the adsorption isotherm, the initial MB concentrations were ranging from 10 to 260 mg/L. After equilibrium is reached, the solutions were centrifuged and the concentration of MB was measured using the following relationship:

$$q_e = \frac{\left(C_0 - C_e\right) \times V}{m} \quad (3)$$

where q_e is the adsorbed MB at equilibrium (mg/g).

3. Results and discussion

3.1. Characterizations of NSW

The proximate and elemental analysis results of NSW show that the adsorbent contains 4.6% moisture, 5.1% ash, and 94.9% fixed carbon. NSW contains low ash content

and high fixed carbon content, which makes it a suitable precursor for activated carbon preparation. The pH_{PZC} of NSW is equal to 6.31. This is an important factor that could affect the interactions mechanism between MB and NSW. The calculated specific surface area of the NSS is 2.49 m^2/g, which is very low compared to that of NSW, which equal to 465.95 m^2/g. It is an important value for NSW as a raw material, which may be due to the extraction of the oil and the release of the pores.

The XRD pattern (Fig. 1a) indicates that NSW material is mainly amorphous with small crystalline domains. The broad peak at 2θ = 22° (plane 002) was attributed to the presence of crystalline cellulose [19,20]. The size of the crystallite determined by Debye–Scherer equation [21] was about 1.5 nm.

The surface chemistry of NSW before and after MB adsorption was evaluated by FTIR (Fig. 1b). The spectrum of NSW shows an absorption band centered at 3,433 cm^{-1} corresponding to the –OH stretching vibrations [22]. The bands of the symmetric and asymmetric stretching of –CH groups are observed at 2,921 and 2,852 cm^{-1} [23]. The band at 1,739 cm^{-1} is assigned to –C=O of ketonic groups [24]. The peaks related to C=O and –NH of amide groups were observed at 1,649 and 1,550 cm^{-1}, respectively. The peak at 1,459 cm^{-1} was attributed to the –C=C stretching, while the peak at around 1,410 cm^{-1} is characteristic of –OH bending of carboxylic groups in NSW [21]. The peak at 1,046 cm^{-1} is related to the –CO stretching vibration of carboxylic, phenolic, and alcoholic groups [25]. After adsorption of MB, new absorption bands at 3,620; 1,516; 930; and 675 cm^{-1} were observed. These bands are attributed to the presence of the dye on NSW. In addition, the intensity of the peaks at 3,433; 2,921; and 1,649 cm^{-1} is significantly reduced. These changes indicated the possible interactions between functional groups present on the surface of NSW (–OH, –COO and $–NH_2$) and MB^+ ions [26].

SEM images of NSW before and after MB adsorption are shown in Fig. 1c. The NSW have a rough surface with a heterogeneous morphology in the presence of protuberances,

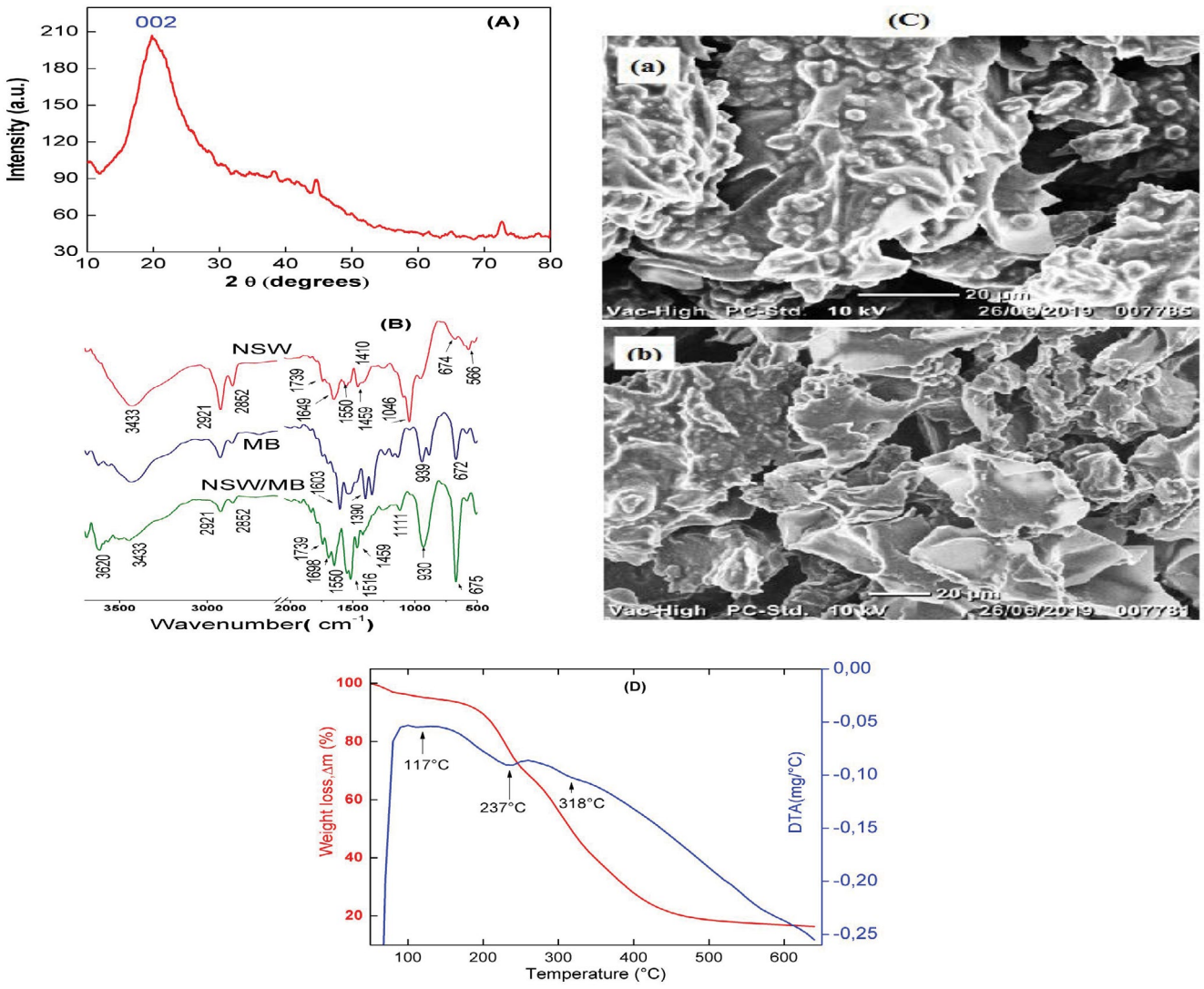

Fig. 1. X-ray diffractogram of NSW (a), FTIR spectra of MB and the adsorbent before (NSW) and after MB adsorption (NSW/MB) (b), SEM images of NSW before (a) and after (b) MB adsorption (c), and TGA-DTA of NSW (d).

cracks and cavities, which offer the NSW high surface area for MB adsorption. After MB adsorption, we observe the appearance of a smooth surface in the form of flowers, which indicates the presence of interactions between the dye and the NSW material.

The thermogravimetric analysis (TGA) of NSW recorded between 30°C and 700°C showed high thermal stability of NSW at 210°C. The initial weight loss (4%), observed around 30°C and 210°C, might be due to the loss of surface adsorbed moisture. While the main weight loss was observed above 210°C due to various dissociation in the carbon framework of NSW. The DTA curve (Fig. 1d) shows 3 endothermic peaks at 117°C, 237°C, and 318°C, related to the dehydration of the sample, the degradation of volatile components such as NSS oil residue and probably the destruction of the carbon to carbon dioxide, respectively [21]. The total weight loss of NSW is approximately 83%.

3.2. Adsorption experiment results

3.2.1. Effect of pH, MB initial concentration, and NSW dose

The pH of the solution is an important factor, which may influence the surface charge of the adsorbent [27]. According to Fig. 2a, the amount of adsorbed MB increased from 2 to 8.5 mg/g when the pH was increased from 2.0 to 4.0. Since the pH_{PZC} of the adsorbent is equal to 6.31, the surface of NSW is positively charged in acidic pH. In addition, the presence of an excess of protons competes with MB cations for the available adsorption sites induces decreasing in MB uptake. However, with the increase of the pH from 4 to 10, the carboxylic acid groups present on the surface of NSW are deprotonated to carboxylate (COO^-), which induce an increase in the electrostatic interactions between NSW surface and MB molecules and therefore an increase in the adsorption capacity [28]. Similar results were obtained by Foo and Hameed [29].

The effect of initial concentration of MB on the adsorption was investigated in the range of C_0 and the results are shown in Fig. 2b. The MB uptake was highly dependent on the initial concentration of the dye. The q_e values increased from 8.3 to 123.3 mg/g with increasing in initial MB concentration from 10 to 256 mg/L due to the acceleration of the mass transfer of MB into the NSW surface [2,9]. However, the removal percentage decreased from 81% to 48% due to the saturation of the NSW surface.

Fig. 2c shows the results of the effect of NSW dose at equilibrium on MB adsorption. The percentage of MB removal increases as the mass of the adsorbent increases because of the availability of important surface area and thus increase in the number of available adsorption sites for MB [30]. The results of the present study showed that 160 mg of NSW could remove 88.7% of MB dye from the solution.

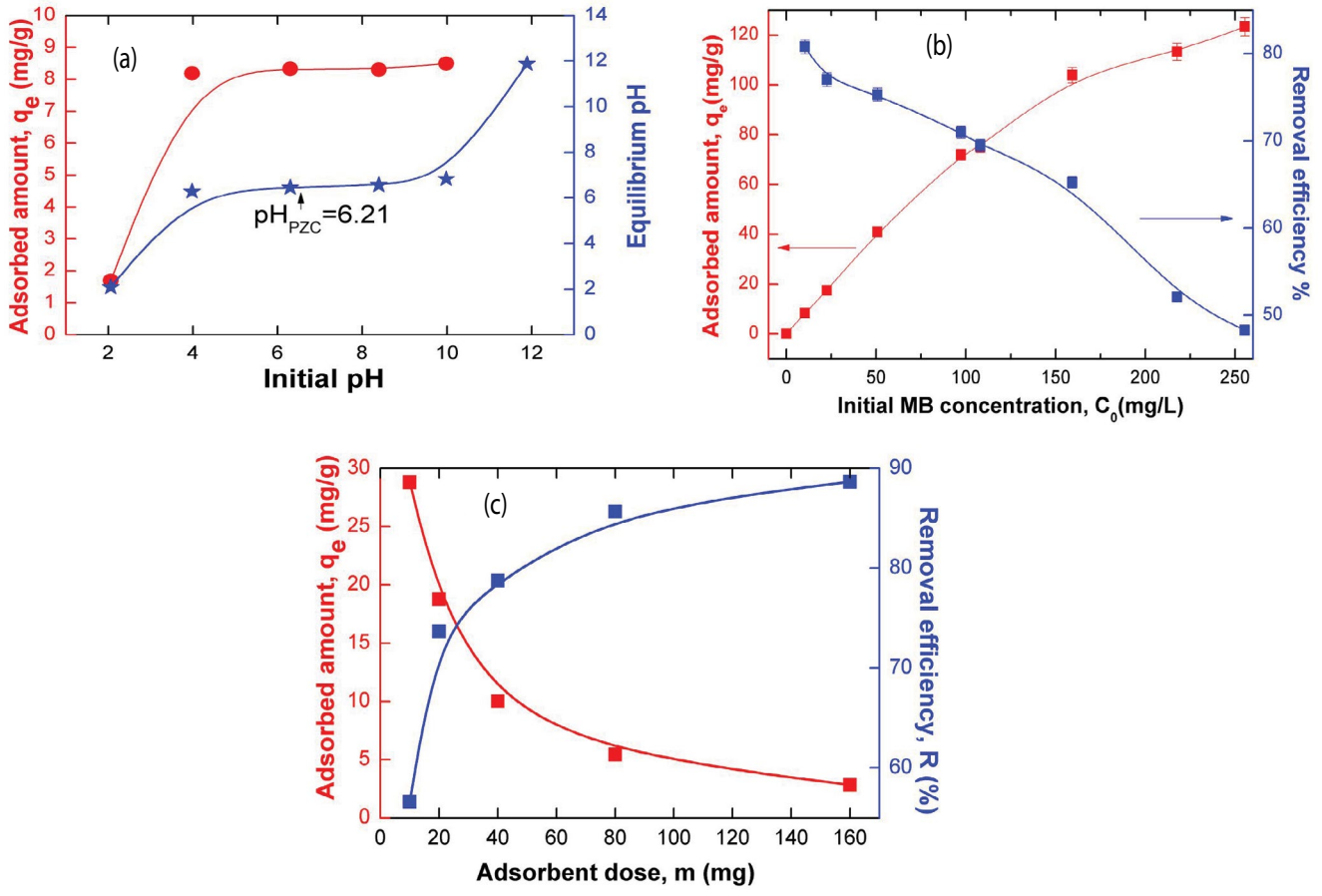

Fig. 2. Effect of pH (a), MB initial concentration (b), NSW dose, and (c) on MB adsorption.

3.2.2. Effect of contact time

The effect of contact time was investigated in the range of the initial MB concentration of 10–60 mg/L. Fig. 3a shows that MB elimination is rapid during the initial stage of contact time and reaches equilibrium in 20 min for all studied concentrations. At the initial contact time, the adsorption was rapid due to the availability of a large number of active sites for MB molecules [30]. After occupying these sites, the adsorption becomes slow. The high MB removal uptake at high concentrations can be attributed to the generation of a gradient of forces created by the gradient of pressure gradient [31].

3.2.3. Kinetic modeling

In order to determine the rate of MB adsorption on NSW, four kinetic models were used: pseudo-first-order [32], pseudo-second-order [33], Avrami [34], and Elovich [35]. These models are represented by the following equations, respectively:

$$q_t = q_e\left(1-\exp\left(-k_1\times t\right)\right) \tag{4}$$

$$q_t = \frac{k_2\times q_e^2\times t}{1+k_2\times q_e\times t} \tag{5}$$

$$q_t = q_e\left(1-\exp\left(-\left(k_{AV}\times t\right)\right)^{n_{AV}}\right) \tag{6}$$

$$q_t = \frac{1}{\beta}\ln\left(\alpha\beta\right)+\frac{1}{\beta}\ln t \tag{7}$$

where k_1 is the rate constant for the pseudo-first-order model (1/min), k_2 is the rate constant for the pseudo-second-order model (g/mg min), k_{AV} (1/min), and n_{AV} are Avrami constants, α (mg/g min) and β (g/mg) are the Elovich coefficients, which represent the initial rate of adsorption and desorption, respectively. The adsorption speed (h_0) for the pseudo-first-order (in mg/g min) and pseudo-second-order models (in mg/g min) can be calculated from the following equations:

$$h_0 = k_1\times q_e \tag{8}$$

$$h_0 = k_2\times q_e^2 \tag{9}$$

The pseudo-first-order model is based on adsorption capacity, while the pseudo-second-order model describes a chemisorption-controlled process. The Avrami model allows the determination of kinetic parameters and the fractional orders if there is a change in the rate of adsorption in the function of the initial concentration and adsorption time. The Elovich model assumes the heterogeneity of adsorption sites and that the process is not influenced by desorption or the interaction of the adsorbate molecules.

Fig. 3a shows the nonlinear fits of the models and Table 1 reports the values of kinetic model parameters. According to R^2 values, the adsorption of MB onto NSW is better described by the Avrami kinetic model at all studied concentrations. In addition, the calculated adsorbed capacities (q_{cal}) by this model are close to the experimental values (q_{exp}). On the other hand, the n_{AV} values show fractional numbers, which means that the adsorption mechanism can follow kinetics with multiple orders that change during the process [36]. The same trends were obtained by Vargas et al. [37].

In order to understand the mechanism of MB adsorption onto NSW, we have used the intraparticle diffusion model (Fig. 3b). This model can be described by the Weber and Morris [38] equation:

$$q_t = k_3\sqrt{t}+C \tag{10}$$

where k_3 is the intraparticle diffusion rate constant (mg/g min$^{0.5}$) and C is the diffusion coefficient. According to the results, the intraparticle diffusion may be involved in the MB adsorption onto NSW in two steps. The first step in the period of $t^{1/2} < 3$ describes the instant adsorption of the dye. The second step, in the range of $3 < t^{1/2} < 16$, is attributed to the slow adsorption until reaching the equilibrium. The k_3 values showed an increase as the concentration increases. The values of the rate constants are between 0.40 and

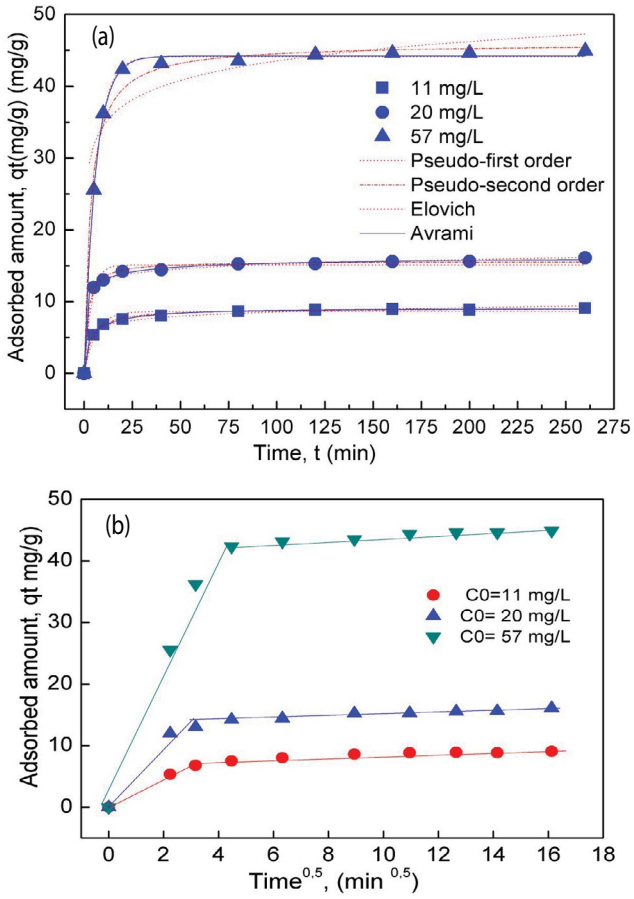

Fig. 3. Effect of contact time on the adsorption of MB onto NSW and kinetics modeling of the process (a) and intraparticle diffusion model of the adsorption of MB onto NSW (b).

Table 1
Kinetic parameters of MB adsorption onto NSW

C_0 (mg/L)	11	20	58
$q_{e,exp}$ (mg/g)	9.1	16.1	44.9
Pseudo-first-order model			
q_e (mg/g)	8.6	15.1	44.2
k_1 (1/min)	0.17	0.28	0.17
h_0	1.46	4.29	7.52
R^2	0.974	0.976	0.998
Pseudo-second-order model			
q_e (mg/g)	9.0	15.6	45.96
k_2 (g/mg/min)	0.032	0.037	0.007
h_0	2.43	9.73	14.81
R^2	0.997	0.994	0.989
Elovich model			
α (mg/g min)	183.64	30,091.4	1.072×10^{42}
β (g/mg)	1.17	1.06	0.26
R^2	0.985	0.996	0.946
Avrami model			
q_e (mg/g)	8.98	16.24	44.2
k_{AV}	0.18	0.67	0.17
n_{AV}	0.456	0.253	0.952
R^2	0.997	0.998	0.998
Intraparticule diffusion model			
k_3	0.40	0.61	1.9
C	4.1	8.3	22.0
R^2	0.554	0.424	0.463

1.9 mg/g $min^{0.5}$. The value of C increases with increase in initial MB concentration due to the boundary layer effect [39].

3.2.4. Adsorption isotherm

The adsorption isotherm study is very important to describe MB-NSW interactions. Adsorption isotherm data were fitted by nonlinear regression analysis using six models: Langmuir [40], Freundlich [41], Temkin [42], Redlich–Peterson [43], Sips [44], and Radke–Prausnitz [45]. These models are presented by the following equations, respectively:

$$q_e = \frac{q_m \times K_L \times C_e}{1 + K_L \times C_e} \tag{11}$$

$$q_e = K_F \times C_e^{1/n} \tag{12}$$

$$q_e = \frac{RT}{b_T} \mathrm{Ln}\left(K_T\, C_e\right) \tag{13}$$

$$q_e = \frac{A_{RP} C_e}{1 + B_{RP} C_e^g} \tag{14}$$

$$q_e = \frac{q_m \times K_S \times C_e^{m_s}}{\left(1 + K_S \times C_e^{m_s}\right)} \tag{15}$$

$$q_e = \frac{q_m \times K_{RP} \times C_e}{\left(1 + K_{RP} \times C_e\right)^{m_{RP}}} \tag{16}$$

where q_m is the maximum adsorption capacity (mg/g), K_L is the Langmuir constant (L/mg), K_F (in (mg/g) $(L/mg)^{1/n}$) and n are Freundlich constants, b_T (kJ/mol) and K_T (L/mol) are Temkin constants, R is the universal gas constant (J/mol.K), T is the temperature (K), A_{GP} (L/mol), B_{RP} (L/mol), and g are constants of Redlich–Peterson model, K_S $((L/g)^{\beta s})$ and m_S are Sips constants, K_{RP} (L/g), and m_{RP} are Radke–Prausnitz constants.

The separation factor R_L of Langmuir model can be used to check whether the adsorption is favorable or not: if $R_L > 1$, the process is not favorable; if $R_L = 1$, the process is linear; if $0 < R_L < 1$, the adsorption is favorable; if $R_L = 0$, the process is irreversible. The separation factor of the Langmuir model (R_L) could be calculated from:

$$R_L = \frac{1}{1 + K_L \times C_0} \tag{17}$$

Adsorption isotherm for MB retention by NSW is presented in Fig. 4. This isotherm indicates the high affinity between MB and NSW surface, particularly at low concentrations. The isotherm is of *L*-type adsorption reaction that represented a system where the adsorbate is strongly attracted by the adsorbent. The values of the maximum adsorbed amount of the dye q_m, the correlation coefficient R^2 and all parameters of all used isothermal models are recorded in Table 2. The value of q_m obtained with the Langmuir model is 149.4 mg/g with the best fit to the experimental data. The R_L value ($0.1 < R_L < 0.75$) indicates favorable adsorption of MB onto NSW (Fig. 4c). The parameter n of the Freundlich model, known as the heterogeneity factor, can be used to identify if the adsorption is linear ($n = 1$), chemical ($n < 1$), or physical ($n > 1$). $1/n < 1$ corresponds to a normal Langmuir isotherm, while if $1/n > 1$, the adsorption is cooperative. The value of n in this study equal to 2.27 and $1/n = 0.44$, indicating the favorable and physical process of MB adsorption onto NSW. The Temkin constant b_T related to the heat of the process is positive and equal to 83.3 kJ/mol, indicating an endothermic process. The Redlich–Peterson isotherm was developed to improve the fit between Langmuir and Freundlich equations. If the value of its parameter $g = 1$, then the Langmuir model is better, if $g = 0$, then the Freundlich model is better. In our case, $g = 1.16$, which indicates that the Langmuir model is more adequate. For Radke–Prausnitz model, the adsorbed quantity $q_m = 197.7$ mg/g, it is greater than that of the Langmuir model. The Sips isotherm is a combination of Langmuir and Freundlich isotherms. The value of q_m of the Sips model is 141.3 mg/g; it is slightly lower than that of the Langmuir model but close to the experimental value. From the analysis of all these isotherms, we conclude that the model of Langmuir is the most plausible to describe the isotherm data of MB adsorption onto NSW. Compared to other materials

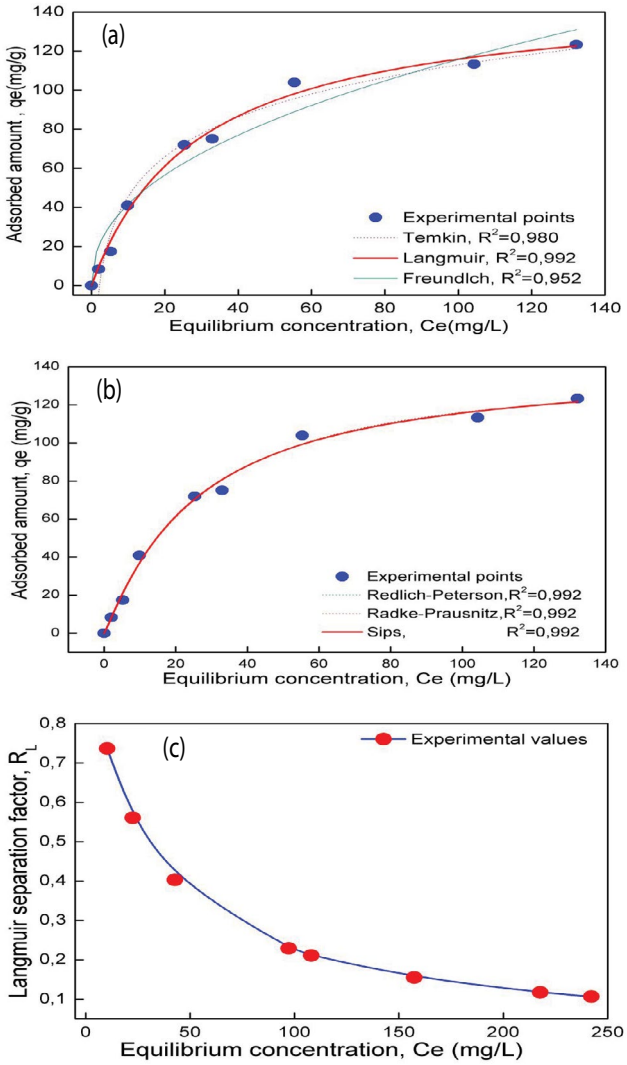

Fig. 4. Nonlinear fits of MB equilibrium adsorption data onto NSW by Temkin, Langmuir, and Freundlich isotherm models (a) and Redlich–Peterson, Sips, and Radke–Prausnitz isotherm models (b), and Langmuir separation factor (c).

listed in Table 3, our unmodified NSW material is considered effective for the removal of MB in the studied concentration range.

3.2.5. Effect of temperature and thermodynamic studies of MB adsorption

The results of the effect of temperature on MB adsorption onto NSW showed that the adsorption capacity increases as the temperature increases (Figure not shown), suggesting that the adsorption reaction is endothermic. This may be due to the increase of dye molecules mobility at high temperature [2]. The variations in standard free energies (Δ*G*°), enthalpy (Δ*H*°), and entropy (Δ*S*°) of MB adsorption were calculated using the following equations [1,2,55]:

$$\Delta G^\circ = -RT\ \mathrm{Ln}K \tag{18}$$

$$\mathrm{Log}\left(\frac{1000\times q_e}{C_e}\right) = \frac{-\Delta H^\circ}{2.303RT} + \frac{\Delta S^\circ}{2.303R} \tag{19}$$

where *R* is the gas constant and *T* is the temperature (K). The slope and the intercept of the Van't Hoff curve is equal to $\frac{-\Delta H^\circ}{2.303R}$ and $\frac{\Delta S^\circ}{2.303R}$, respectively.

The calculated thermodynamic parameters (Table 4) shows the positive value of the enthalpy (Δ*H*°=15.1 kJ/mol) indicating the endothermic MB adsorption onto NSW. Since this value is less than 40 kJ/ mol, the interactions between MB molecules and the NSW surface are physical. The values of Δ*G*° at different temperatures are –15.4, –16.4, and –17.4 kJ/mol indicating that the adsorption process is spontaneous and inversely proportional to the temperature [56–57]. The positive value of the entropy (Δ*S*°=103.9 J/mol K) confirmed the spontaneous adsorption of MB onto NSW, and indicate the disorderliness adsorption process at the adsorbent surface.

Table 2
Langmuir, Freundlich, Temkin, Redlich–Person, Radke–Prausnitz, and Sips parameters for MB adsorption onto NSW

Langmuir	q_m (mg/g)	b (L/mg)		R^2
	149.4	0.035		0.993
Freundlich	K_F (mg/g)(L/mg) $^{1/n}$	n		R^2
	14.93	0.44		0.952
Temkin	b_T (kJ/mol)	K_T (L/mol)		R^2
	83.3	0.475		0.980
Redlich–Peterson	A_{RP} (L/mol)	B_{RP} (L/mol)	g	R^2
	4.51	0.013	1.16	0.998
Radke–Prausnitz	K_{RP}	q_m	m_{RP}	R^2
	0.024	197.7	1.15	0.992
Sips	q_m (mg/g)	K_S	m_S	R^2
	141.3	0.028	0.91	0.992

Table 3
Maximum adsorption capacity of NSW and other adsorbents for MB

Adsorbent	C_0 (mg/L)	q_{max}(mg/g)	Model	Reference
Almond shell	100–1,000	51.02	Freundlich	[46]
Peanut husk	80	72.13	Temkin	[47]
Apricot stones-AC	5–100	36.68	Langmuir	[48]
Camelina-derived	10–100	5.08	Langmuir/Freundlich	[49]
Sapindus-derived	10–100	50.76	Langmuir/Freundlich	[49]
Sumac leaves	2–7	5.80	Langmuir/Temkin	[50]
Water bamboo leaves	50–250	54.17	Langmuir	[51]
Walnut shell	20–100	51.55	Langmuir	[52]
Potato (*Solanum tuberosum*) peel	10–40	14.83	Langmuir	[53]
Modified *Nigella sativa* seeds	–	194	Langmuir	[54]
Nigella sativa seeds waste	5–260	149.4	Langmuir	This study

Table 4
Thermodynamics of MB adsorption onto NSW

Temperature (K)	Thermodynamics		
	$\Delta H°$ (kJ/mol)	$\Delta S°$(J/mol K)	$\Delta G°$(kJ/mol)
293			–15.4
303	15.1	103.9	–16.4
313			–17.4

3.2.6. Statistical physics analysis

The Langmuir model has been successfully applied in several liquid and gas adsorption systems, but this model presents disadvantages. Among them, the interactions between the adsorbed molecules are ignored and so this model has been revised in several publications using statistical physics processing. The model of statistical physics in relation to ideal gas theory has recently been developed. It represents the general case of the model assuming that each site on the adsorbent surface can accept n adsorbate molecules [58]. The model can be described by the following equation:

$$q_e = \frac{n \times N_M}{1 + \left(\frac{C_{1/2}}{C_e}\right)^n} \tag{20}$$

where n is the number of adsorbed molecules per site, $C_{1/2}$ (mg/L) is the concentration at half saturation, N_M (mg/g) is the receptor site density, q_e (mg/g) is the adsorbed amount, and C_e (mg/L) is the concentration at equilibrium.

The adsorbed dye quantity at saturation (N_{sat}) can be calculated by:

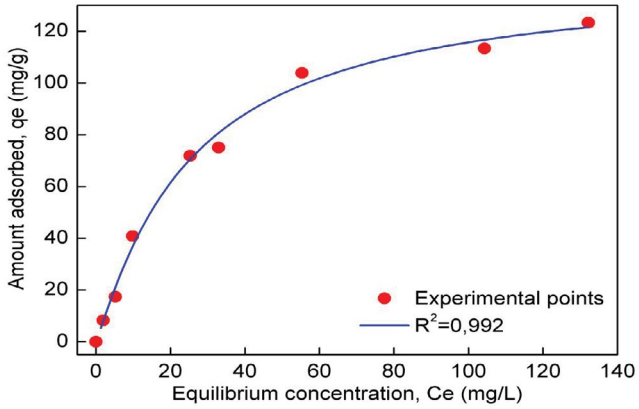

Fig. 5. MB adsorption isotherm fitting by the monolayer model.

$$N_{sat} = nN_M \tag{21}$$

According to the literature [59], the number n indicates the position of adsorbed molecules onto the surface of the adsorbent. The application of the model to the experimental data is shown in Fig. 5. According to R^2 values (Table 5), there is a good correlation between the model and the experimental data with n = 1.10. This suggests the perpendicular orientation and the anchorage of MB molecules on the surface of NSW. The N_M and N_{sat} are 128.23 and 141.1 mg/g, while $C_{½}$ is 25.4 mg/L.

The interactions between MB molecules and NSW surface could be explained through the adsorption energy estimation from the equation:

$$\Delta E = RT \ \mathrm{Ln}\left(\frac{C_s}{C_0}\right) \tag{22}$$

Table 5
Statistical physics parameters for MB adsorption onto NSW

Parameters	n	N_m	q_{sat} (mg/g)	$C_{1/2}$ (mg/L)	ΔE (kJ/mol)
Value	1.10	128.34	141.1	25.4	18.0

where C_s is the solubility of MB and $C_{1/2}$ is the calculated half saturation concentration. The value of the adsorption energy is 18.0 kJ/mol, indicating the endothermic and physical nature of MB adsorption. Similar results were obtained by Toumi et al. [59] for the adsorption of MB onto agricultural waste.

4. Conclusion

In this study, NSW were simply prepared and used for MB removal from water. The results indicated that NSW were efficient for MB adsorption under the effect of different experimental conditions such as pH, temperature, NSW dose, and initial MB concentration. The kinetics of the adsorption process followed the Avrami model. Moreover, the intraparticle diffusion study proved that MB was adsorbed on two stages. The isotherm equilibrium data were described by the Langmuir isotherm model with a maximum adsorption capacity of 144.8 mg/g, while the monolayer model suggested the multimolecular process and the physical adsorption of MB onto NSW.

Acknowledgments

The authors thank the Laboratory of Chemical Engineering (LGPC) and the University of Setif, Algeria for the financial support.

References

[1] N. Boukhalfa, M. Boutahala, N. Djebri, A. Idris, Kinetics, thermodynamics, equilibrium isotherms, and reusability studies of cationic dye adsorption by magnetic alginate/oxidized multiwalled carbon nanotubes composites, Int. J. Biol. Macromol., 123 (2019) 539–548.
[2] N. Djebri, M. Boutahala, N.E. Chelali, N. Boukhalfa, L. Zeroual, Adsorption of bisphenol A and 2.4.5-trichlorophenol onto organo-acid-activated bentonite from aqueous solutions in single and binary systems, Desal. Water Treat., 66 (2017) 383–393.
[3] C. Duran, D. Ozdes, A. Gundogdu, H.B. Senturk, Kinetics and isotherm analysis of basic dye adsorption onto almond shell (*Prunus dulcis*) as a low cost adsorbent, J. Chem. Eng. Data, 56 (2011) 2136–2147.
[4] J.M. Salman, V.O. Njoku, B.H. Hameed, Adsorption of pesticides from aqueous solution onto banana stalk activated carbon, Chem. Eng. J., 174 (2011) 41–48.
[5] M. Ahmaruzzaman, S.I. Gayatri, Activated tea waste as a potential low-cost adsorbent for the removal of p-nitrophenol from wastewater, J. Chem. Eng. Data, 55 (2010) 4614–4623.
[6] J.M. Salman, B.H. Hameed, Effect of preparation conditions of oil palm fronds activated carbon on adsorption of bentazon from aqueous solutions, J. Hazard. Mater., 175 (2010) 133–137.
[7] A. Altunsik, E. Gur, Y. Seki, A natural sorbent, *Luffa* cylindrical for the removal of a model basic dye, J. Hazard. Mater., 179 (2010) 658–664.
[8] I. Ali, M. Asim, T.A. khan, Low cost adsorbents for the removal of organic pollutants from wastewater, J. Environ. Manage., 113 (2012) 170–183.
[9] M.J. Ahmed, S.K. Theydan, Equilibrium isotherms and kinetics modeling of methylene blue adsorption on agricultural waste-based activated carbons, Fluid Phase Equilib., 317 (2012) 9–14.
[10] S. De Gisi, G. Lofrano, M. Grassi, M. Notarnicola, Characteristics and adsorption capacities of low-cost sorbents for wastewater treatment: a review, Sustainable Mater. Technol., 9 (2016) 10–40.
[11] Y. Zhou, L. Zhang, Z. Cheng, Removal of organic pollutants from aqueous solution using agricultural wastes: a review, J. Mol. Liq., 212 (2015) 739–762.
[12] Z. Gholamnezhad, S. Havakhah, M.H. Boskabady, Preclinical and clinical effects of *Nigella sativa* and its constituent, thymoquinone: a review, J. Ethnopharmacol., 190 (2016) 372–386.
[13] A. Nasir, M. Siddiqui, M. Mohsin, Therapeutic uses of shoneez (*Nigella sativa* Linn.) mentioned inunani system of medicine: a review, Int. J. Pharm. Phytopharmacol. Res., 4 (2014) 47–49.
[14] A. Ahmad, A. Husain, M. Mujeeb, S.A. Khan, A.K. Najmi, N.A. Siddique, Z.A. Damanhouri, F. Anwar, A review on therapeutic potential of *Nigella sativa*: a miracle herb, Asian Pac. J. Trop. Biomed., 3 (2013) 337–352.
[15] M. Mahboubi, Natural therapeutic approach of *Nigella sativa* (black seed) fixed oil in management of sinusitis, Integr. Med. Res., 7 (2018) 27–32.
[16] C.K.C. Bedin, I.P.A.F. Sousa, A.L. Cazetta, L. Spessato, A. Ronix, V.C. Almeida, CO_2-spherical activated carbon as a new adsorbent for methylene blue removal: kinetic, equilibrium and thermodynamic studies, J. Mol. Liq., 269 (2018) 132–139.
[17] B.K. Nandi, A. Goswami, M.K. Purkait, Adsorption characteristics of brilliant green dye on kaolin, J. Hazard. Mater., 161 (2009) 387–395.
[18] K.M. Kifuani, A.K.K. Mayeko, P.N. Vesituluta, B.I. Lopaka, G.E. Bakambo, B.M. Mavinga, J.M. Lunguya, Adsorption d'un colorant basique, Bleu de Méthylène, en solution aqueuse, sur un bioadsorbant issu de déchets agricoles de *Cucumeropsis mannii* Naudin, Int. J. Biol. Chem. Sci., 12 (2018) 558–575.
[19] R. Gong, Y. Sun, J. Chen, H. liu, C. Yang, Effect of chemical modification on dye adsorption capacity of peanut hull, Dyes Pigm., 67 (2005) 175–181.
[20] C. Djilani, R. Zaghdoudi, A. Modarressi, M. Rogalski, F. Djazi, A. Lallam, Elimination of organic micropollutants by adsorption on activated carbon prepared from agricultural waste, Chem. Eng. J., 189–190 (2012) 203–212.
[21] S.I. Siddiqui, S.A. Chaudhry, *Nigella sativa* plant based nanocomposite-$MnFe_2O_4$/BC: antibacterial material for water purification, J. Cleaner Prod., 200 (2018) 996–1008.
[22] G. Shams Khorramabadi, R. Darvishi Cheshmeh Soltani, A. Rezaee, A.R. Khataee, A. Jonidi Jafari, Utilization of immobilised activated sludge for the biosorption of Chromium(VI), Can. J. Chem. Eng., 90 (2012) 1539–1546.
[23] A. Gundogdu, C. Duran, H.B. Senturk, M. Soylak, M. Imamoglu, Y. Onal, Physicochemical characteristics of a novel activated carbon produced from tea industry waste, J. Anal. Appl. Pyrolysis, 104 (2013) 249–259.
[24] B. Hameed, F. Daud, Adsorption studies of basic dye on activated carbon derived from agricultural waste: *Hevea brasiliensis* seed coat, Chem. Eng. J., 139 (2008) 48–55.
[25] S. Norouzi, M. Heidari, V. Alipour, O. Rahmanian, M. Fazizadeh, F. Mohammadi-Moghadam, H. Nourmoradi, B. Goudarzi, K. Dindarloo, Preparation, characterization and Cr(IV) adsorption evaluation of NaOH-activated carbon produced from date Press cake; an agro-industrial waste, Bioresour. Technol., 258 (2018) 48–56.
[26] A. Nasrullah, B. Saad, A.H. Bhat, A. Sada Khan, M. Danish, M. Hasnain Isa, A. Naeem, Mangosteen peel waste as a sustainable precursor for high surface area mesoporous activated carbon: characterization and application for methylene blue removal, J. Cleaner Prod., 211 (2019) 1190–1200.
[27] S.I. Siddiqui, S. Ali Chaudhry, nanohybrid composite Fe_2O_3-ZrO_2/BC for inhibiting the growth of bacteria and adsorptive removal of arsenic and dyes from water, J. Cleaner Prod., 223 (2019) 849–868.
[28] S.I. Siddiqui, G. Rathi, S.A. Chaudhry, Acid washed black cumin seed powder preparation for adsorption of methylene blue dye from aqueous solution: thermodynamic, kinetic and isotherm studies, J. Cleaner Prod., 264 (2018) 275–284.
[29] K. Foo, B. Hameed, Preparation, characterization and evaluation of adsorptive properties of orange peel based activated carbon via microwave induced K_2CO_3 activation, Bioresour. Technol., 104 (2012) 679–686.
[30] Y. Zhou, J. Lu, Y. Zhou, Y. Liu, Recent advances for dyes removal using novel adsorbents: a review, Environ. Pollut., 252 (2019) 352–365.

[31] A. Benhouria, M. Azharul Islam, H. Zaghouane-Boudiaf, M. Boutahala, B.H. Hameed, Calcium alginate–bentonite–activated carbon composite beads as highly effective adsorbent for methylene blue, Chem. Eng. J., 270 (2015) 621–630.
[32] S. Largergren, On the theory of so-called adsorption of solutes, Kungl. Sven. Vetenskapsakad. Handl., 24 (1898)1–39.
[33] Y.S. Ho, G. McKay, Pseudo-second-order model for sorption processes, Process Biochem., 34 (1999) 451–465.
[34] M. Avrami, Kinetics of phase change: transformation-time relations for random distribution of nuclei, J. Chem. Phys., 8 (1940) 212–224.
[35] C. Aharoni, M. Ungarish, Kinetics of activated chemisorptions. Part I: the non-Elovichian part of the isotherm, J. Chem. Soc., Faraday Trans 1., 72 (1976) 265–268.
[36] E.C.N. Lopes, F.S.C. dos Anjos, E.F.S. Vieira, A.R. Cestari, An alternative Avrami equation to evaluate kinetic parameters of the interaction of Hg(II) with thin chitosan membranes, J. Colloid Interface Sci., 263 (2003) 542–547.
[37] A.M.M. Vargas, A.L. Cazetta, M.H. Kunita, T.L. Silva, V.C. Almeida, Adsorption of methylene blue on activated carbon produced from flamboyant pods (*Delonix regia*): study of adsorption isotherms and kinetic models, Chem. Eng. J., 168 (2011) 722–730.
[38] W.J. Weber, J.C. Morris, Kinetics of adsorption on carbon from solution, J. Sanitary Eng. Div., 89 (1963) 31–60.
[39] O.S. Bello, M.A. Ahmad, N. Ahmad, Adsorptive features of banana (*Musa paradisiaca*) stalk-based activated carbon for malachite green dye removal, Chem. Ecol., 28 (2012) 153–167.
[40] I. Langmuir, The constitution and fundamental properties of solids and liquids, J. Am. Chem. Soc., 38 (1916) 2221–2295.
[41] H.M.F. Freundlich, Uber die adsorption in loesungen, Z. Phys. Chem., 57 (1906) 385–470.
[42] M. Hadi, M.R. Samarghandi, G. Mckay, Equilibrium two-parameter isotherms of acid dyes sorption by activated carbons: study of residual errors, Chem. Eng. J., 160 (2010) 408–416.
[43] O. Redlich, D.L. Peterson, A useful adsorption isotherm, J. Phys. Chem., 63 (1959) 1024.
[44] R. Sips, combined form of Langmuir and Freundlich equations, J. Chem. Phys., 16 (1948) 490–495.
[45] C.J. Radke, J.M. Prausnitz, Adsorption of organic solutes from dilute aqueous solution on activated carbon, Ind. Eng. Chem. Fundam., 11 (1972) 445–451.
[46] C. Duran, D. Ozdes, A. Gundogdu, H.B. Senturk, Kinetics and isotherm analysis of basic dyes adsorption onto almond shell (*Prunus dulcis*) as a low cost Adsorbent, J. Chem. Eng. Data, 56 (2011) 2136–2147.
[47] J. Song, W. Zou, Y. Bian, F. Su, R. Han, Adsorption characteristics of methylene blue by peanut husk in batch and column modes, Desalination, 265 (2011) 119–125.
[48] C. Djilani, R. Zaghdoudi, F. Djazi, B. Bouchekima, A. Lallam, A. Modarressi, M. Rogalski, Adsorption of dyes on activated carbon prepared from apricot stones and commercial activated carbon, J. Taiwan Inst. Chem. Eng., 53 (2015) 112–121.
[49] S. Sharma, D. Tiwari, K. Pant, Model-fitting approach for methylene blue dye adsorption on *Camelina* and *Sapindus* seeds-derived adsorbents, Adsorpt. Sci. Technol., 34 (2016) 565–580.
[50] J. Gülen, B. Akın, M. Özgür, Ultrasonic-assisted adsorption of methylene blue on sumac leaves, Desal. Water Treat., 57 (2016) 9286–9295.
[51] L. Zhu, Y. Wang, T. He, L. You, X. Shen, Assessment of potential capability of water bamboo leaves on the adsorption removal efficiency of cationic dye from aqueous solutions, J. Polym. Environ., 24 (2016) 148–158.
[52] R. Tang, C. Dai, C. Li, W. Liu, S. Gao, C. Wang, Removal of methylene blue from aqueous solution using agricultural residue walnut shell: equilibrium, kinetic, and thermodynamic studies, J. Chem., 2017 (2017) 1–10, doi: 10.1155/2017/8404965.
[53] E.K. Guechi, O. Hamdaoui, Biosorption of methylene blue from aqueous solution by potato (*Solanum tuberosum*) peel: equilibrium, modeling, kinetic, and thermodynamic studies, Desal. Water Treat., 57 (2016) 10270–10285.
[54] S. Rakass, A. Mohmoud, H. Oudghiri Hassani, M. Abboudi, F. Kooli, F. Wadaani, Modified *Nigella sativa* seeds as a novel efficient natural adsorbent for removal of methylene blue dye, Molecules, 23 (2018) 1950.
[55] E.C. Lima, A.H. Bandegharaei, I. Anastopoulos, Response to "some remarks on a critical review of the estimation of the thermodynamic parameters on adsorption equilibria. Wrong use of equilibrium constant in the van't Hoff equation for calculation of thermodynamic parameters of adsorption, J. Mol. Liq., 273 (2019) 425–434.
[56] J. Gülen, F. Zorbay, Methylene blue adsorption on a low cost adsorbent – carbonized peanut shell, Water Environ. Res., 89 (2017) 805–816.
[57] J. Gülen, M. İskeçeli, Removal of methylene blue by using porous carbon adsorbent prepared from carbonized chestnut shell, Mater. Test., 59 (2017) 188–194.
[58] L. Sellaoui, G.L. Dotto, E.C. Peres, Y. Benguerba, E.C. Lima, A. Ben Lamine, A. Erto, New insights into the adsorption of crystal violet dye on functionalized multi-walled carbon nanotubes: experiments, statistical physics and COSMO-RS models application, J. Mol. Liq., 248 (2017) 890–897.
[59] K.H. Toumi, Y. Benguerba, A. Erto, G.L. Dotto, M. Khalfaoui, C. Tiar, S. Nacef, A. Amrane, Molecular modeling of cationic dyes adsorption on agricultural Algerian olive cake waste, J. Mol. Liq., 264 (2018) 127–133.